Available online at www.sciencedirect.com

SCIENCE DIRECT

Surface & Coatings Technology 200 (2006) 3690–3697

SURFACE & COATINGS TECHNOLOGY

www.elsevier.com/locate/surfcoat

Annealing behavior of electrodeposited Ni-TiO_2 composite coatings

C.S. Lin[a,*], C.Y. Lee[b], C.F. Chang[b], C.H. Chang[b]

[a]*Department of Materials Science and Engineering, National Taiwan University, 1 Roosevelt Road, Section 4 Taipei 106, Taiwan*
[b]*Department of Mechanical and Automation Engineering, Da-Yeh University Changhua 515, Taiwan*

Received 31 August 2004; accepted in revised form 1 October 2004
Available online 5 November 2004

Abstract

The properties of nickel-ceramic composite electrodeposits are greatly influenced by the type and amount of ceramic particles in the deposit and the microstructure of the nickel matrix. In the present study, Ni-TiO_2 coatings were electroplated in the nickel sulfamate bath containing 50 g l^{-1} TiO_2. Results show that TiO_2 codeposited in nickel led to the formation of nanocrystalline nickel grains surrounding the TiO_2 particle and the increase in crystalline defects such as twins, dislocations and grain boundaries. These defects, on one hand, enhanced the hardness of the Ni-TiO_2 coating and, on the other hand, reduced the recrystallization temperature of nickel. Nevertheless, codeposited TiO_2 effectively inhibited the growth of recrystallized nickel grains. And yet, the hardness of the composite coating dropped drastically after annealing at temperatures higher than 600 °C due to the relatively large voids formed by the reaction of TiO_2 particles with nickel.

Keywords: Electroplating; Nickel sulfamate; Ni-TiO_2 composite coating; Nanocrystalline nickel; Recrystallization

1. Introduction

Electrodeposition of ceramic, polymer and metal particles within metal matrix produces composite coatings with the attractive properties such as high wear resistance, corrosion resistance and electrocatalysis [1–5]. Since these properties are strongly governed by the volume fraction of the particles codeposited in the coating, many efforts have been made to correlate the amount of codeposited particles to the process parameters. These parameters include the bath composition and the concentration of suspended particles in the bath; the particle form, size and size distribution; the addition of surfactant and metallic ions; and the electroplating parameters such as temperature, pH, the type of imposed current, current density, and the type and degree of agitation [2–20].

Extensive studies have been conducted to understand the codeposition mechanism of inert particles from electrolyte baths and the strategies for enhancing the amount of codeposited particles. Guglielmi [6] formulates the first theoretical model based on the mechanism involving two successive adsorption steps and shows that the amount of particles codeposited in the metal matrix can be related to the current density and the concentration of particles suspended in the bath. Since then, the codeposition of inert particles with metal electrodeposits from the distinct baths has usually been explained based on adsorption of metal ions on the particles [6–14]. For example, the inert particles, once adsorbing metal ions, acquire positive surface charges and are potentially adsorbed on the electrode surface. Further reduction of these metal ions results in strong adsorption of the particles onto the metal matrix. Other than the effects of ion adsorption, agitation has been shown to play a significant role in the codeposition of inert particles in metal electrodeposits [7,15,16]. Based on the knowledge of the flow field around an electrode and all of the forces acting on a particle, a trajectory model has been employed to

* Corresponding author. Tel.: +886 2 3366 5240; fax: +886 2 2363 4562.
E-mail address: csclin@ntu.edu.tw (C.S. Lin).

0257-8972/$ - see front matter © 2004 Elsevier B.V. All rights reserved.
doi:10.1016/j.surfcoat.2004.10.001

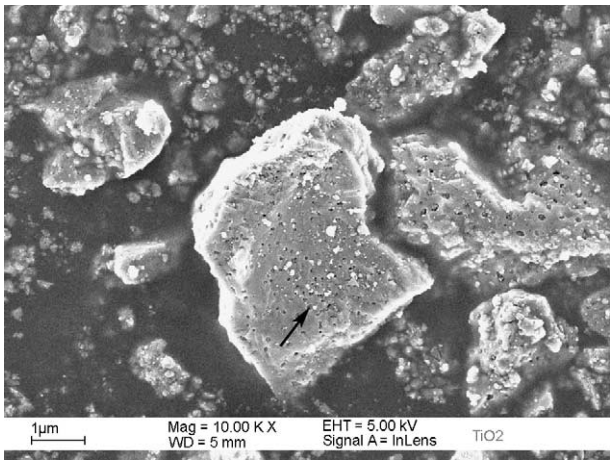

Fig. 1. SEM micrograph showing the morphology, shape and size distribution of the TiO_2 particles.

estimate the particle codeposition rate [15,16]. Finally, certain additive [2,18–20] and metal cations [8–10,14,17] in the bath can effectively increase the amount of the codeposited particles.

Although there is plenty of literature concerning the effects of bath composition and operation conditions on the amount of inert particles codeposited in the metal matrix and the resulting properties of the composite coatings, little is known about the effect of codeposited particles on the microstructure and annealing behavior of the composite coating. It has been shown that nickel ions in a sulfamate bath are readily adsorbed on to the surface of titania [6,7]. Furthermore, since the isoelectric point of titania is about pH 5.7 [21], protons are potentially adsorbed onto titania particles suspended in the conventional nickel sulfamate bath with a pH of around 4. The titania with adsorption of either protons or nickel ions becomes positively charged and can be codeposited within nickel during electroplating. The present study demonstrates that TiO_2 particles are codeposited in nickel from a nickel sulfamate bath without addition of particular additives. Furthermore, codeposited TiO_2 particles modify the grain structure and lattice defects of the nickel matrix, which in turn affect the annealing behavior of the composite coating.

2. Experimental details

In the present study, both pure nickel and Ni-TiO_2 composite coatings were galvanostatically plated onto a copper substrate in a nickel sulfamate bath at 50 °C with a current density of 1000 A m^{-2}. Prior to electroplating, the copper plates were polished with emery paper up to grade 2400, rinsed in distilled water and, finally, activated in 5% sulfuric acid at room temperature. The basic sulfamate solution was made up of 95 g l^{-1} nickel ions as nickel sulfamate, 40 g l^{-1} boric acid, 3 g l^{-1} nickel chloride and 0.4 g l^{-1} sodium dodecyl sulfate (anti-pitting agent). The pH of the solution was adjusted to 4 using either sulfamate acid or dilute sodium hydroxide solution. To prepare the composite coating, 50 g l^{-1} TiO_2 powders (rutile of 99% purity, Alfa, Johnson Matthey) with an average size reported to be 2–3 μm by the manufacturer were suspended in the basic solution. The microstructure of these TiO_2 powders is shown in Fig. 1. A wide range of particle size distribution was observed. The typical size of the particles was around 2–3 μm, while the particles with sizes in nanometer to submicron range were also observed. Moreover, many nanosized voids (marked as the arrow in Fig. 1) were frequently observed in the particles. These voids must have formed during the production of the powders although no details on the manufacturer's processing method have been given. Electroplating was performed using a plating cell consisting of a vertical anode and cathode separated by a distance of 10 mm. The solution with suspended TiO_2 particles was circulated by pumping throughout electroplating. The thickness of the deposits was controlled to be approximately 70 μm by the plating time for a specific current density. Both the pure nickel and Ni-TiO_2 coatings were annealed in air at temperatures of 300, 400, 600 and 800 °C for 2 h.

The structure of various deposits was first examined using cross-sectional metallography specimens. The volume percent of codeposited TiO_2 and the grain size of the nickel matrix before and after annealing were measured using LECO 2001 image analysis system. A combined mechanical grinding and ion-beam thinning technique was employed to prepare the cross-sectional transmission electron microscope (TEM) specimens. The defect structure of the composite coating was characterized using the selected-area diffraction technique and nanobeam diffraction technique. Additionally, the composition of the alloy layer formed at the TiO_2/Ni interface after annealing was measured via energy-dispersive spectrometry (EDS) in TEM using an electron probe of 10 nm in diameter. Finally, the hardness of pure nickel and composite coatings was

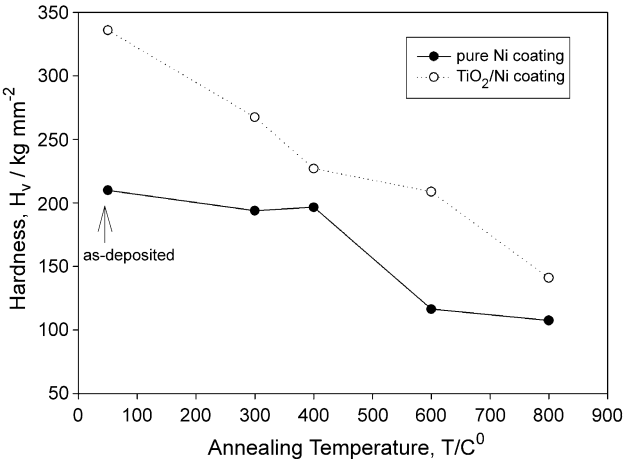

Fig. 2. Hardness of the pure nickel and Ni-TiO_2 coatings as a function of the annealing temperature.

measured on the polished cross sections with an applied load of 50 g. The hardness of each deposit was reported as an average of eight measurements. Both the hardness measurement and cross-sectional TEM characterization were performed at the center of the cross sections to avoid the influence of the surface oxide layer and the Ni–Cu alloy layer formed via interdiffusion during high-temperature annealing. For example, after 2 h of annealing at 800 °C, the thickness was approximately 5 and 25 μm for the former and the latter, respectively, as measured by the electron probe microanalysis (not shown here).

3. Results and discussion

3.1. Deposit hardness

Fig. 2 shows the hardness of nickel and Ni-TiO_2 composite coatings as a function of the annealing temperature. The hardness of the as-deposited Ni-TiO_2 coating was approximately 340 kg mm^{-2}, which is approximately 50% larger than that of the pure nickel coating. Furthermore, the hardness of this composite coating is comparable to that of nanocrystalline nickel electrodeposits [22,23]. Upon annealing, the hardness of the Ni-TiO_2 coating decreased continuously with increasing annealing temperature. In contrast, the hardness of the nickel coating showed little change up to 2 h of annealing at 400 °C, followed by a rapid decrease as the annealing temperature was increased to 600 °C. Although the deposit hardness change differed from the distinct coatings, the Ni-TiO_2 coating was harder than the nickel counterpart regardless of the annealing temperature. This result indicates that codeposited TiO_2 particles in the nickel matrix enhanced the strength of the coating, especially for the as-deposited coating and that annealed at 600 °C (Fig. 2).

3.2. Deposit microstructure

Fig. 3 illustrates the changes in the grain structure of the pure nickel coating with the annealing temperature. As shown in Fig. 3a, the nickel coating exhibited a columnar grain structure when cross-sectionally observed under an optical microscope. Fig. 3b and c shows that the nickel coating still consisted of columnar grains after 2 h of annealing at 300 and 400 °C, respectively. The little change

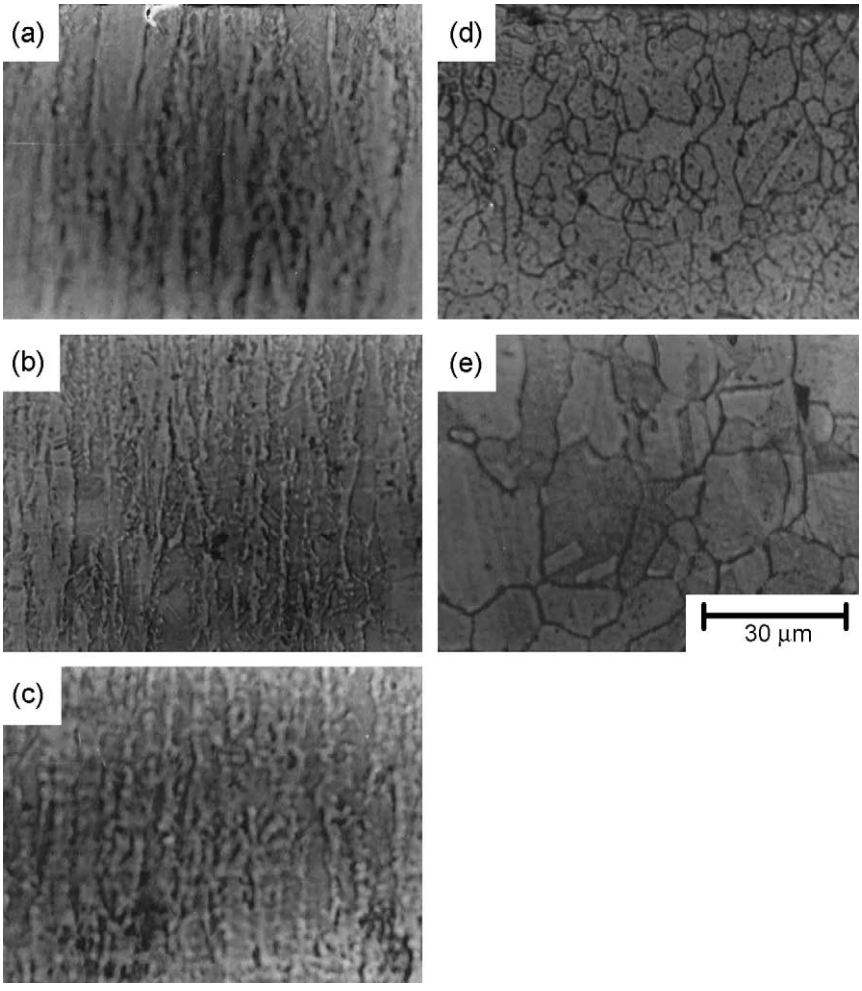

Fig. 3. Cross-sectional optical micrographs of nickel coatings: (a) as-deposited, and after 2 h of annealing at (b) 300, (c) 400, (d) 600 and (e) 800 °C.

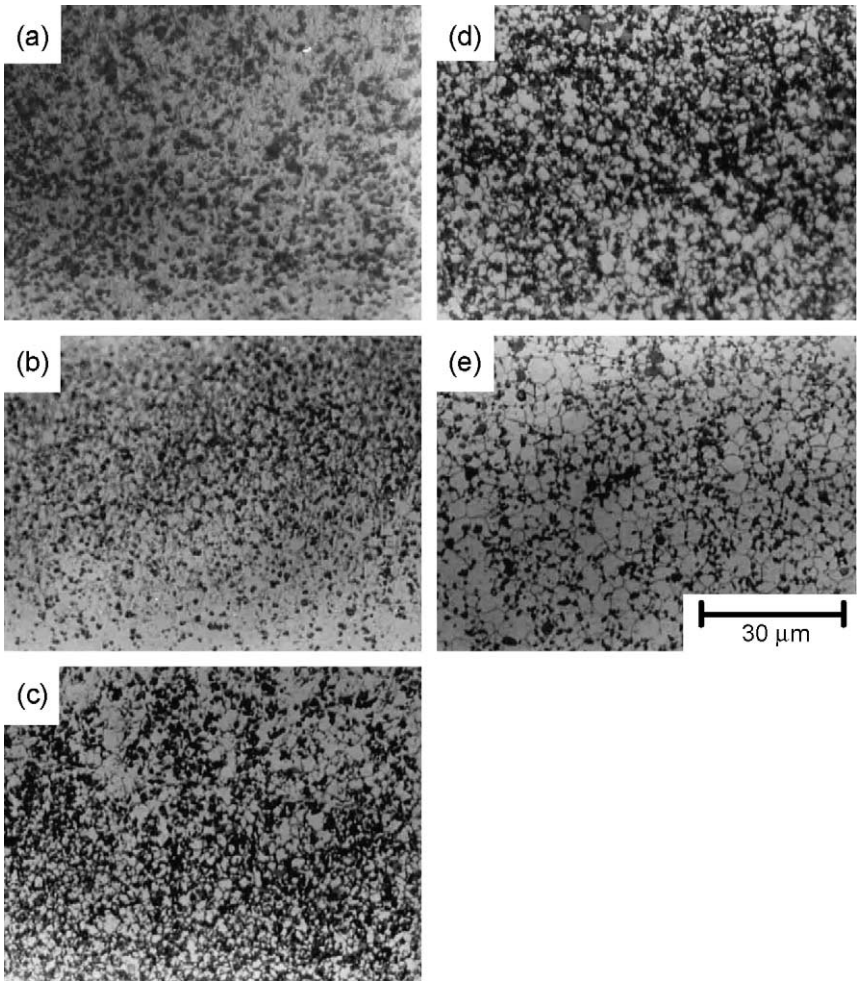

Fig. 4. Cross-sectional optical micrographs of Ni-TiO_2 coatings: (a) as-deposited, and after 2 h of annealing at (b) 300, (c) 400, (d) 600 and (e) 800 °C.

in grain structure accounted for the slight hardness change associated with the nickel coating annealed up to 400 °C. Recrystallization and grain growth were observed on the nickel coating (Fig. 3d) when the annealing temperature was increased to 600 °C, thereby causing an abrupt drop in the deposit hardness. Further increasing the annealing temperature to 800 °C resulted in a softer nickel coating comprising relatively large grains (Fig. 3e).

Fig. 4a shows that approximately 15% (in volume) of TiO_2 was uniformly codeposited within nickel when 50 g l^{-1} TiO_2 powders were added to the basic nickel sulfamate solution. This observation agrees well with those reported in Refs. [6,7] that prepared Ni-TiO_2 coatings from simple nickel sulfamate baths. However, none of these studies investigated the effect of TiO_2 particles on the structure of the nickel matrix. Fig. 4a also shows that codeposited TiO_2 notably refined the grain structure of nickel, which was too fine to be resolved via the traditional optical metallography [24]. After 2 h of annealing at 300 °C, recrystallized grains were observed on the Ni-TiO_2 coating (Fig. 4b). The formation of recrystallized grains led to a significant decrease in the deposit hardness (Fig. 2). Further increase in the annealing temperature resulted in continuous grain growth of the Ni-TiO_2 coating (Fig. 4c, d and f). Fig. 5 shows the dependence of the nickel grain size on the annealing temperature for pure nickel and Ni-TiO_2 coatings. In this figure, the size of columnar nickel was defined as the

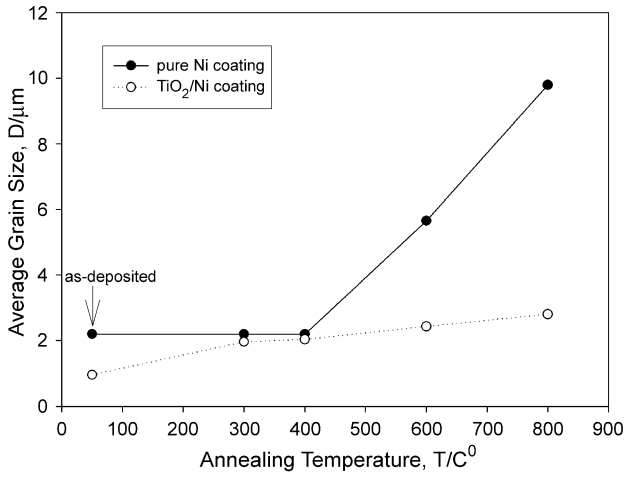

Fig. 5. Average grain size of the nickel matrix as a function of the annealing temperature.

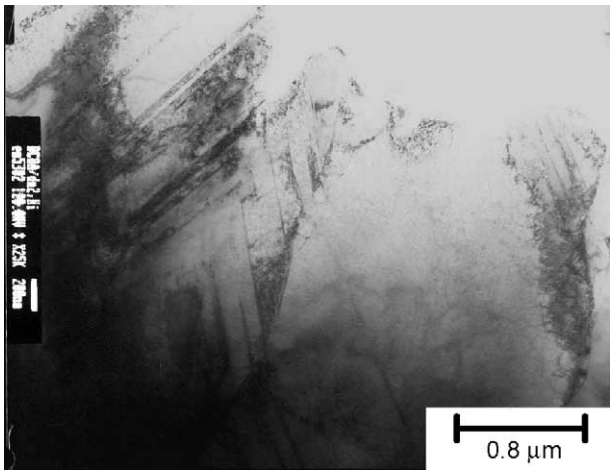

Fig. 6. Cross-sectional TEM micrograph of the as-deposited nickel coating.

average width of the columnar grains, while that of recrystallized grains was the average of their diameters. As shown in Fig. 5, the average width of columnar nickel showed little change after annealing at 400 °C. In contrast, nickel grains grew substantially with increasing annealing temperature after recrystallization. The nickel grains of the Ni-TiO_2 coating annealed at 300 °C had an average size of 1.96 μm, which was approximately two times the size of the as-deposited coating, namely 0.96 μm. Fig. 5 also shows that, once recrystallized, the nickel grain growth rate of the Ni-TiO_2 coating was significantly lower than that of the nickel coating. Codeposited TiO_2 apparently retards the growth of the nickel grains. This retardation effect is due to the impedance on grain boundary migration by the TiO_2 particles residing along the grain boundaries of the nickel grains (Fig. 8). The observation will be further explained later.

The pure nickel coating was further characterized by cross-sectional TEM. Fig. 6 shows that the as-deposited nickel coating consisted of coarse columnar grains of which column axes were along the direction of the electric field imposed during electroplating. Furthermore, crystalline defects, such as dislocations and twins, were observed in the nickel grains. The twin plane was usually at an angle of between 25 and 35° with respect to the axis of columnar nickel grains. In addition to the columnar grains, a cluster of equiaxed grains was occasionally observed (not shown here). Our previous study [25] demonstrated that the density of the twin defects in the nickel coating determines the recrystallization behavior of the coating plated from the nickel sulfamate solution. For example, the nickel deposit with [110] texture has a high density of twins whose twin planes notably remain parallel to the axis of the columnar grain and undergoes recrystallization and grain growth after 1 h of annealing at 400 °C. In contrast, the nickel deposit with strong [100] texture contains less amount of twins as compared with its [110] counterpart and suffers grain growth in the absence of recrystallization after 1 h of annealing up to 600 °C. The result that the pure nickel coating contains fewer twins and still retains its columnar grain structure up to 400 °C annealing for 2 h further confirms that the density of the twins plays a major role in recrystallization of the nickel coating.

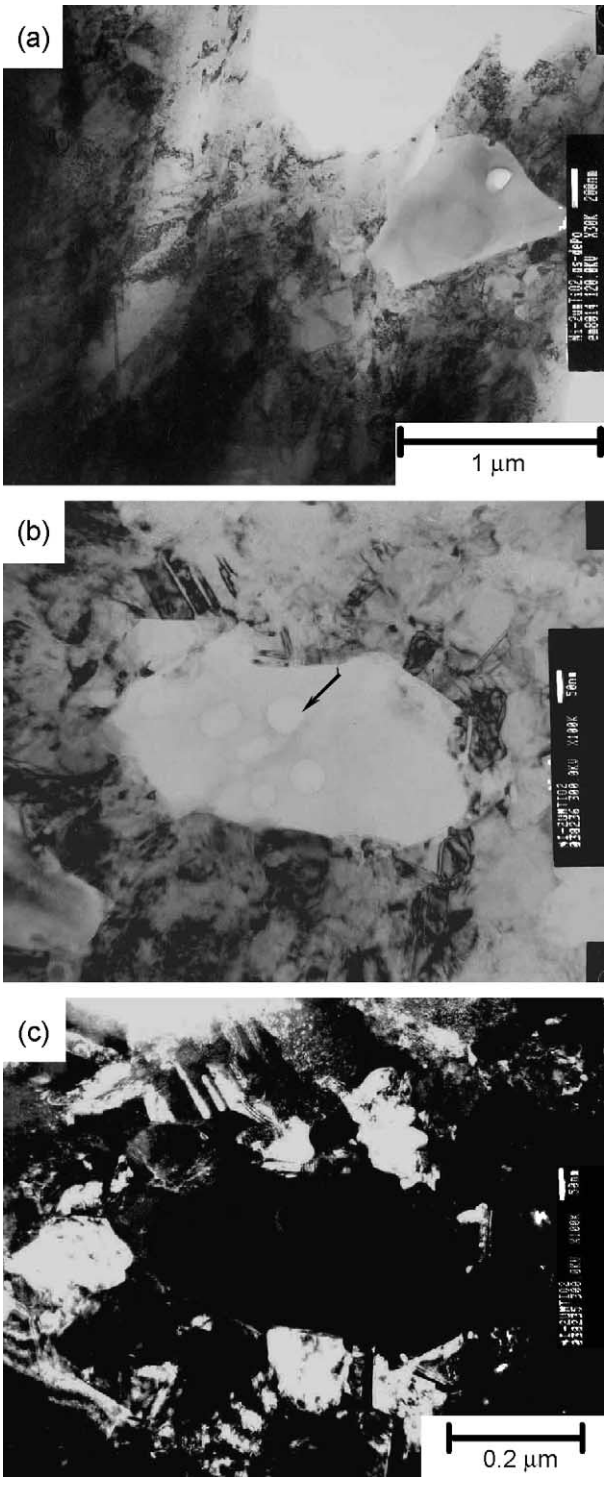

Fig. 7. Cross-sectional TEM micrographs of the as-deposited Ni-TiO_2 coating: (a) the overall columnar structure of the composite coating, (b) a close-up view around a TiO_2 particle showing the equiaxed nanocrystalline nickel grains surrounding a TiO_2 particle and (c) the dark-field image shown in (b) illustrating twins present in the nanocrystalline nickel grains.

Fig. 7a shows that the Ni-TiO_2 coating also exhibited a columnar grain structure. The nickel grains contained a high density of lattice defects such as twins and dislocations. Except the columnar nickel matrix, the TiO_2 particle was usually surrounded by a cluster of equiaxed nanocrystalline nickel grains (Fig. 7b and c). Fig. 7b further reveals the existence of nanosized voids (marked by the arrow) in TiO_2, in consistent with the SEM observation (Fig. 1). Moreover, twins were also observed in these nanocrystalline nickel grains (Fig. 7c). An explanation for the formation of the nanocrystalline nickel grains can be related to adsorption and subsequent reduction of the ions adsorbed on TiO_2 particles that are weakly bonded at the nickel/solution interface. In a nickel sulfamate bath, the major cations adsorbed on TiO_2 particles are protons and Ni^{2+} ions. Discharge of protons results in both the atomic and molecular forms of hydrogen. Both prohibit the lateral growth of nickel electrodeposits, but favor the development of [110] and [210] textures, which are known as the inhibited growth mode associated with nickel electrodeposits [28,29]. Reduction of Ni^{2+} ions adsorbed on TiO_2 particles forms an electric conductive layer covering the particles. The applied electric field can then be concentrated on these weakly adsorbed particles since they act as protrusions at the moving interface between nickel and the solution (see Fig. 2 in Ref. [6]). Nucleation rate of nickel is enhanced at these particles at which the local current density is relatively large. Probably, enhanced nucleation and inhibited growth of nickel on TiO_2 particles lead to the formation of equiaxed nanocrystalline nickel grains. Other as yet unidentified factors can also play a significant role in the formation of nanocrystalline nickel grains.

After 2 h of annealing at 400 °C, the columnar nickel grains of the Ni-TiO_2 coating were completely replaced by equiaxial recrystallized grains. Furthermore, most of the TiO_2 particles were observed to reside along the boundaries of the new grains (Fig. 8a). The reaction between nickel grains and TiO_2 particles was also noted with the reaction fronts moving into the TiO_2 particle (as marked by the arrow in Fig. 8b). This reaction resulted in voids at the reaction fronts. These voids tended to grow and merge each other to form a large hole as the annealing temperature was further increased. Fig. 9a shows that a TiO_2 particle was partly replaced by sizable holes (indicated by the arrow); thereby the TiO_2 particle was disintegrated into several relatively small TiO_2 grains. A close-up view (Fig. 9b) further reveals that these relatively small TiO_2 grains were encased by a nickel-rich oxide layer composed of nickel, titanium and oxygen species (Fig. 9d). The breakdown of the TiO_2 particle and the encasement of each relatively small TiO_2 grain with a nickel-rich oxide layer suggest the primary reaction between the TiO_2 particle and nickel matrix at high temperatures should be resulted from the diffusion of nickel into the TiO_2 particle. Such diffusion can be enhanced by the pre-existing voids in the TiO_2 particle. The formation mechanism of the hole during high-temperature annealing, however, remains to be determined.

Introducing TiO_2 particles to the nickel matrix leads to an increase in the deposit hardness. The nanocrystalline nickel grains surrounding TiO_2 particles further contribute to the hardness of the deposit. Consequently, the Ni-TiO_2 coating has hardness similar to that of nanocrystalline nickel electrodeposits [22,23]. The Ni-TiO_2 coating, although is harder than its nickel counterpart, undergoes recrystallization at a lower temperature. In contrast, the pure nickel coating consisting of relatively coarse columnar grains has better thermal stability than the Ni-TiO_2 coating. Czerwinski and Szpunar [26] prepared the microcrystalline and nanocrystalline nickel deposited from a Watts bath and noted that the nickel deposits with uniform grains in micrometer have a higher thermal stability than those with nanocrystalline grains or with a mixture of microcrystalline and nanocrystalline grains. Therefore, the lower recrystallization temperature associated with the Ni-TiO_2 coating is presumably due to its high defect density such as twins, Ni-TiO_2

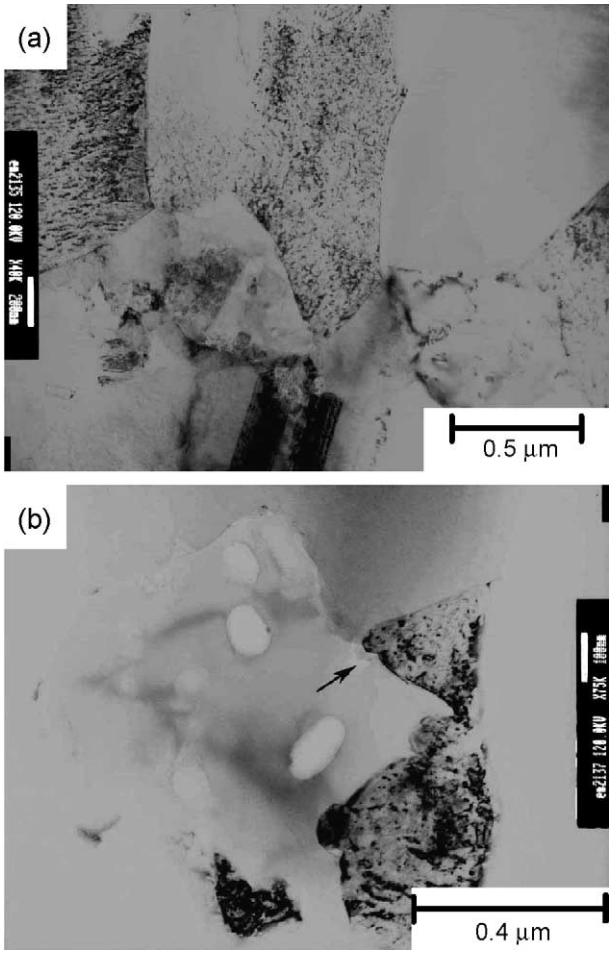

Fig. 8. Cross-sectional TEM micrographs of the Ni-TiO_2 coating annealed at 400 °C for 2 h: (a) the TiO_2 particles residing at the grain boundaries of recrystallized nickel grains and (b) a close-up view around a TiO_2 particle showing the reaction fronts between nickel matrix and TiO_2.

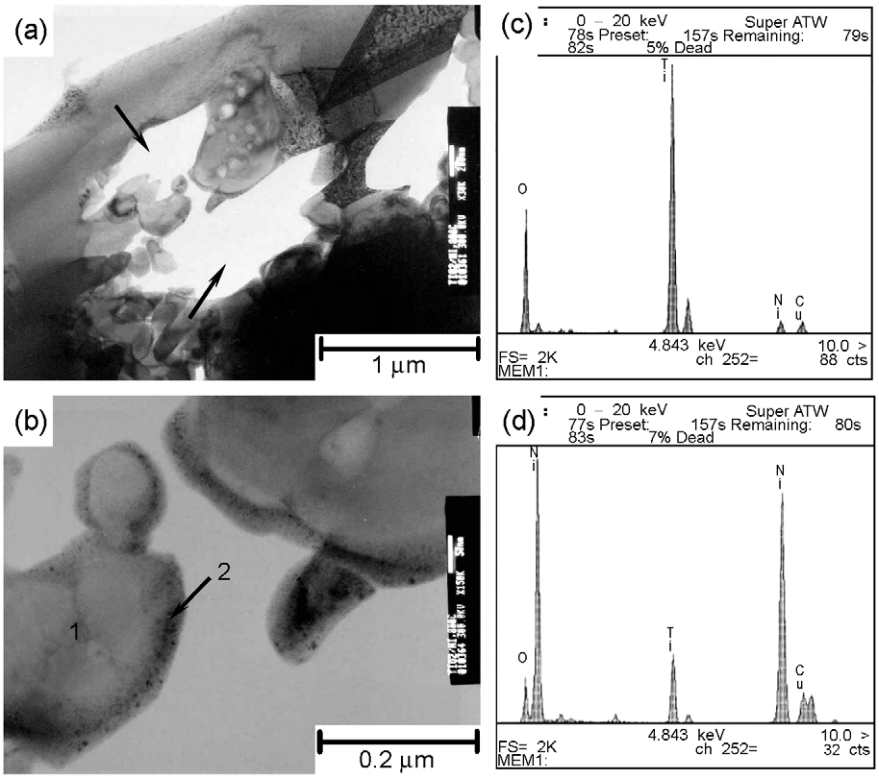

Fig. 9. Cross-sectional TEM micrographs of the Ni-TiO_2 composite coating annealed at 800 °C for 2 h: (a) relatively large holes in a TiO_2 particle, (b) a close-up view showing encasement of the relatively small TiO_2 grains with a nickel-rich oxide layer, and (c and d) the EDS spectrums taken from the areas marked as 1 and 2 in Fig. 9b, respectively.

interfaces and nickel grain boundaries, particularly the boundaries between nanocrystalline nickel grains. Unlike the nanocrystalline nickel electrodeposits that exhibit abnormal grain growth at temperatures exceeding 280 °C [27], the impedance in nickel grain growth by the TiO_2 particles benefits the high-temperature hardness of the coating. A composite electrodeposit with TiO_2 particles, preferably nanoparticles, dispersed in nanocrystalline nickel matrix might be an ideal material for high-temperature application since codeposited TiO_2 can prohibit abnormal growth of nanocrystalline nickel. However, it needs to be noted that the formation of voids within the TiO_2 particles at temperatures higher than 600 °C significantly deteriorates the hardness of the Ni-TiO_2 composite coating.

4. Conclusions

Ni-TiO_2 composite coating was electroplated from a nickel sulfamate bath containing 50 g l^{-1} TiO_2 particles. The composite coating was strengthened by the incorporated TiO_2 particles and the nanocrystalline nickel grains surrounding the TiO_2 particles. The formation of nanocrystalline nickel grains was related to the reduction of the cations adsorbed on the surface of the TiO_2 particles, namely discharge of protons and reduction of Ni^{2+} ions.

The pure nickel coating consisted of columnar grains of which defect density was lower than that of the Ni-TiO_2 coating. Accordingly, the grain structure and hardness of the nickel coating hardly changed after 2 h of annealing at 400 °C. On the contrary, the Ni-TiO_2 coating exhibited recrystallization after annealing at 300 °C. This lower crystallization temperature associated with the Ni-TiO_2 coating was due to its higher density of lattice defects, particularly the boundaries between nanocrystalline nickel. Nevertheless, the TiO_2 particles effectively inhibited the growth of the nickel grains by residing themselves on the grain boundaries of the recrystallized nickel grains. And yet, such a inhibition in nickel grain growth could not prevent the deposit from softening as the annealing temperature was increased from 600 to 800 °C, when many relatively large holes formed within the TiO_2 particles.

Acknowledgements

The authors would like to thank the National Science Council of the Republic of China for financially supporting this research under grant no. 902216E212001. Ms. L.C. Wang, National Sun Yat-sen University, is recognized for her assistance with the TEM work. This study made use of the Electron Microscopes of National Sun Yat-sen Univer-

sity and National Taiwan University, supported by the National Science Council, Republic of China.

References

[1] M. Musiani, Electrochim. Acta 45 (2000) 3397.
[2] K. Helle, F. Walsh, Trans. IMF 75 (2) (1997) 53.
[3] I. Garcia, J. Fransaer, J.-P. Celis, Surf. Coat. Technol. 148 (2001) 171.
[4] A. Takahashi, Y. Miyoshi, T. Hada, J. Electrochem. Soc. 141 (1994) 954.
[5] C. Maeda, T. Mega, J. Himomura, S. Kurokawa, J. ISIJ 82 (1996) 69.
[6] N. Guglielmi, J. Electrochem. Soc. 119 (1972) 1009.
[7] A.M.J. Kariapper, J. Foster, Trans. IMF 52 (1974) 87.
[8] J.P. Celis, J.R. Roos, J. Electrochem. Soc. 124 (1977) 1508.
[9] J.R. Roos, J.P. Celis, J.A. Helsen, Trans. IMF 55 (1977) 113.
[10] C. White, J. Foster, Trans. IMF 56 (1978) 92.
[11] M.J. Bhagawat, J.P. Celis, J.R. Roos, Trans. IMF 61 (1983) 72.
[12] K. Nishimura, Y. Miyoshi, T. Hada, Jap. J. Surf. Technol. 38 (1987) 217.
[13] B.J. Hwang, C.S. Hwang, J. Electrochem. Soc. 140 (1993) 979.
[14] K.-M. Yin, H.J. Hong, Trans. IMF 75 (1997) 35.
[15] J. Fransaer, J.P. Celis, J.R. Roos, J. Electrochem. Soc. 139 (1992) 413.
[16] J. Fransaer, J.P. Celis, J.R. Roos, Metal Finish. 91 (6) (1993) 97.
[17] T.W. Tomaszewski, L.C. Tomaszewski, H. Brown, Plating 56 (1969) 1234.
[18] N.K. Shrestha, I. Miwa, T. Saji, J. Electrochem. Soc. 148 (2001) C106.
[19] L. Benea, P.L. Bonora, A. Borello, S. Martelli, F. Wenger, P. Ponthiaux, J. Galland, J. Electrochem. Soc. 148 (2001) C461.
[20] S.C. Wang, W.C. Wei, Mater. Chem. Phys. 78 (2003) 574.
[21] S.G.J. Heijmand, H.N. Stein, Langmuir 11 (1995) 422.
[22] F. Ebrahimi, G.R. Bourne, M.S. Kelly, T.E. Matthews, Nanostruct. Mater. 11 (1999) 343.
[23] N.S. Qu, D. Zhu, K.C. Chan, W.N. Lei, Surf. Coat. Technol. 168 (2003) 123.
[24] C.S. Lin, K.C. Peng, P.C. Hsu, L. Chang, C.H. Chen, Trans. JIM 41 (2000) 777.
[25] C.S. Lin, P.C. Hsu, K.C. Peng, L. Chang, C.H. Chen, Trans. JIM 42 (2001) 316.
[26] F. Czerwinski, J.A. Szpunar, Nanostruct. Mater. 11 (1999) 669.
[27] N. Wang, Z. Wang, K.T. Aust, U. Erb, Acta Mater. 45 (1997) 1655.
[28] J. Amblard, M. Froment, G. Maurin, Electrodep. Surf. Treat. 2 (1973/74) 205.
[29] J. Amblard, I. Epelboin, M. Froment, G. Maurin, J. Appl. Electrochem. 9 (1979) 233.